Influence of Interpass Temperature on Wire Arc Additive Manufacturing (WAAM) of Aluminium Alloy Components

Karan Derekar[1,2,*], *Jonathan* Lawrence[1], *Geoff* Melton[3], *Adrian* Addison[3], *Xiang* Zhang[1] and *Lei* Xu[3]

[1]Faculty of Engineering, Environment and Computing, Coventry University, Coventry, UK
[2]National Structural Integrity Research Centre (NSIRC Ltd.), Granta Park, Great Abington, Cambridge, UK
[3]TWI, Granta Park, Great Abington, Cambridge, UK

Abstract. Wire arc additive manufacturing (WAAM) technique has revealed the potential of replacing existing aerospace industry parts manufactured by traditional manufacturing routes. The reduced mechanical properties compared to wrought products, the porosity formation, and solidification cracking are the prime constraints that are restricting wide-spread applications of WAAM products using aluminium alloys. An interpass temperature is less studied in robotic WAAM and is the vital aspect affecting the properties of a formed product. This paper highlights the effects of change in interpass temperature on porosity content and mechanical properties of WAAM parts prepared using DC pulsed GMAW process, with 5356 aluminium consumable wire. The samples prepared with different interpass temperatures were studied for the distribution of pores with the help of computed tomography radiography (CT radiography) technique. A WAAM sample produced with higher interpass temperature revealed 10.41% less porosity than the sample prepared with lower interpass temperature. The pores with size less than 0.15mm3 were contributing over 95% of the overall porosity content. Additionally, on a volumetric scale, small pores (<0.15mm3) in the higher interpass temperature sample contributed 81.47% of overall volume of pores whereas only 67.92% volume was occupied in lower interpass temperature sample with same sized pores. The different solidification rates believed to have influence on the hydrogen evolution mechanism. Tensile properties of higher interpass temperature sample were comparatively better than lower interpass temperature sample. For the deposition pattern used in this study, horizontal specimens were superior to vertical specimens in tensile properties.

1 Introduction

Inherent process capabilities of low buy-to-fly ratio, high deposition rate and theoretically no dimensional limits are responsible for making wire arc additive manufacturing (WAAM) a promising technique. Its suitability for medium to large scale parts production with low to medium complexity [1] is one of the appealing aspects for many researchers. High cost materials such as Ti-6Al-4V and Inconel 625 and 718 which are preferred choices for aero-engine parts are highly experimented with WAAM. The reason being low cost manufacturing process that not only reduces overall production time but also the wastage of material.

Aluminium alloys find widespread applications in the transportation and aerospace industries. This has propelled the applications of parts produced using WAAM technique due to the lead time; however inherent metal properties such as solidification cracking, porosity formation and reduced mechanical properties at the weld and heat affected zone (HAZ) are the determinants that are restricting its full-fledged application. An application of the cold metal transfer (CMT) mode and interlayer rolling have provided positive solutions to minimise and even eliminate the porosity [2], [3].

Interpass temperature in welding has always been a crucial issue. The adverse effect of interpass temperature on the microstructure as well as on mechanical properties of the weld is widely studied. Many researchers have discussed in detail the microstructures of an object formed through layer deposition [4]–[6]. However, the effect of interpass temperature on material properties is not studied thoroughly. While manufacturing an additively manufactured object, an attention is usually given to the inter bead dwell time [2], [7]–[9] through robotic programming. The temperature of the top deposited layer immediately before deposition of next layer is not considered. A deposition of material in a layered format with specific time interval progressively increases the temperature [10] and thermal stresses [11] of a formed part and thus eventually an interpass temperature through heat sink effect. The effects of heat sink and heat extraction techniques were exercised [12]–[14] and respective mechanical and microstructural properties were studied. Geng et al. [12] outlined improved bead geometry for increased interpass temperatures ranging from 50°C to 120°C and unacceptable beads over 150°C. The presented results support BS EN 1011-4:2000 that restricts interpass temperature at 120°C for similar filler chemistry.

Predominant problem of porosity formation during aluminium welding was discussed by many researchers. A wide difference in the solubility of hydrogen in liquid and solid aluminium (0.036cm3/100g in solid against 0.69cm3/100g in liquid at a melting point of 660°C) is

* Corresponding author: derekark@uni.coventry.ac.uk

responsible for pore formation. A study on pore formation on work hardenable aluminium alloy when 3D deposition format was considered, Gu et al. [9] claimed the presence of volatile metals, specifically Mg, was responsible for the formation and growth of the pores. Mathers [15] raised a concern about the lack of knowledge in regards the effect of loss of volatile metals (Mg and Ti) during welding on the strength of the weld, as Mg represents a strength raiser in 5xxx series alloys.

Grain orientation affects the tensile strength of an additively manufactured objects. Geng et al. [16] while studying a single bead multi wall structure, showed the differences in the tensile properties of an object when load was applied in longitudinal and transverse directions with respect to the grain orientation. Another study focusing on the microstructure variations, Cong et al. [17] disclosed transition of grain structure from columnar to cellular structure at the bottom, equiaxed non-dendritic at the central region and equiaxed dendritic at the top section of an additively manufactured thin wall. However, the block structure revealed transition of grain structure within a single layer, equiaxed non-dendritic at middle and equiaxed dendritic at the outer part. Further, comparatively higher heat sink in a block structure compared to wall was the reason for the presence of different microstructures.

There hardly any work published that highlights the inter-relation between interpass temperature and properties of an additively manufactured part. The aim of the paper is to highlight the effects of interpass temperature on the amount and distribution of porosity, mechanical and microstructural properties of a block structure prepared using work hardenable aluminium alloy through pulsed MIG/MAG process.

2 Experimental procedure

2.1 Material and consumables

To study the effects of interpass temperature on additively manufactured aluminium alloy samples, thick wall samples were manufactured using DC pulsed MIG/MAG process. A power source for metal deposition was OTC Welbee 500. ER5356 filler wire of 1.2 mm diameter was employed for the study. The nominal chemical composition of filler wire is given in Table 1. A substrate of comparable chemistry with dimensions 250 x 100 x 25 mm was used. The weld pool was shielded using pure argon gas with a gas flow rate of 20 l/min.

Table 1. Nominal chemical composition of Al5356 filler wire

Si	Mn	Cr	Cu	Ti	Zn	Fe	Mg
<0.25	0.15	0.13	<0.05	0.11	<0.1	<0.4	5

2.2 Deposition of the wall samples

The pattern of metal deposition during the fabrication of wall samples is depicted in Figure 1. Details of the welding and torch oscillating parameters deployed during the wall formation are given in Table 2. In-built linear torch oscillating function was selected for this study. The interpass temperatures maintained during the building of two walls were 50 and 100°C and the wall samples are referred as Wall-1 and Wall-2 respectively in further discussion of this paper.

For the first layer, substrates were preheated up to 50 and 100°C for Wall-1 and Wall-2 respectively which is considered as preheat temperature and for all subsequent layers, predefined temperature was maintained thorough out the deposition time. A digital thermometer was used for temperature measurement. Only, a temperature of the top layer was considered as a depositing criteria for the deposition of successive layer. The temperature of substrate and all other surfaces of the wall was not considered in this paper because the study is directed towards the pore formation which is surface phenomena and the effect of temperature distribution in the WAAM part is widely studied for the formation and distribution of residual stresses. It is emphasised that a substrate and four surfaces of wall samples showed considerable difference in temperature with respect to the top surface of the wall samples. Approximately 45 layers were deposited with each layer height 3mm. Figure 2 illustrates the additively manufactured aluminium wall sample with dimensions 190 × 135 × 45 mm^3.

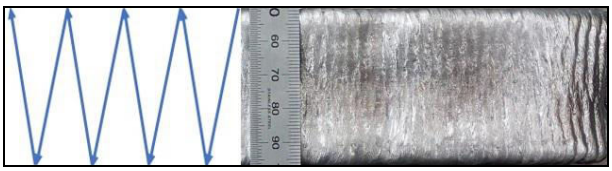

Fig. 1. Pattern of metal deposition applied for wall fabrication (photograph shows the thickness of wall)

Table 2. Welding parameters used during part fabrication

Parameters	Values
Welding details	
Base current (A) for low pulse	60
Peak current (A) for low pulse	275
Base current (A) for high pulse	100
Peak current (A) for high pulse	290
Wave frequency (Hz)	20
Wave ratio (%)	35
Linear torch travel speed (mm/m)	60
Torch Oscillation	
Frequency (Hz)	0.3
Mode	Linear
Amplitude (mm)	40
Dwell time (sec)	0.1 at ¼ and ¾ and 0 at ½

2.3 Testing

After building of wall samples, Computed Tomography (CT) radiography was performed to examine the distribution and amount of pores present in the walls. Initially, complete wall structures were radiographed. Later, walls were sectioned through 70mm from one end and then re-radiographed for the smaller section.

After completion of non-destructive testing, three vertical and three horizontal round tensile test specimens were extracted from each wall. Figure 3 illustrates approximate positions of the tensile specimens within a wall. Tensile load tests were carried out at room temperature complying with BS EN ISO 6892-1:2016 to generate full stress-strain curves from round shaped specimens. For the microstructural observation specimens were obtained from the locations described in Figure 3 and a routine procedure was followed to prepare a suitable specimens. Initially, specimens were mounted, followed by polishing operation on 120, 320, 600, 1200, 2500 and 4000 grade polishing papers. Electron microscopy was used for the observation and recording of microstructural variations.

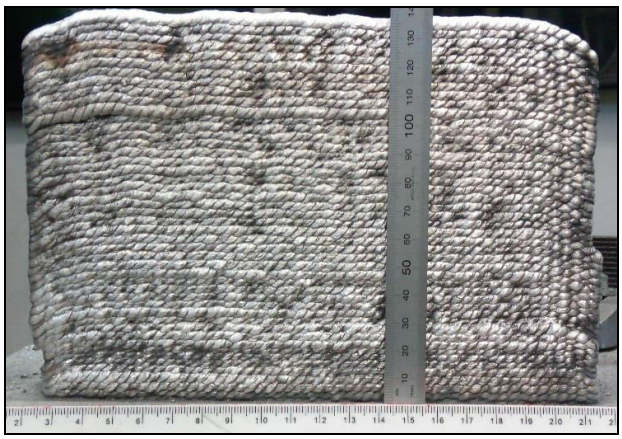

Fig. 2. Photograph of an additively manufactured aluminium wall made of Al 5356 wire. Two walls were built using interpass temperature values of 50°C (Wall-1) and 100°C (Wall-2)

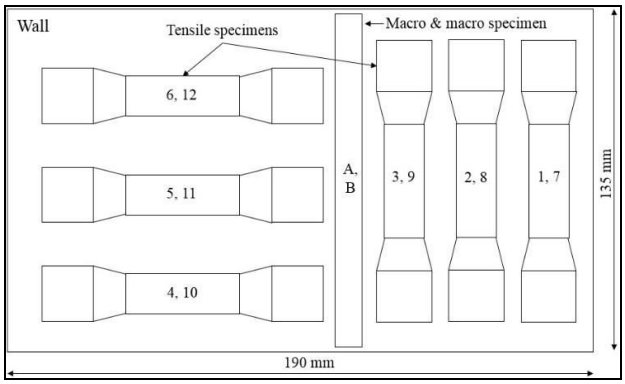

Fig. 3. Location of test specimens from Wall 1 (50°C) and Wall 2 (100°C) respectively. Specimen 1 to 6 were extracted from Wall-1 and 7 to 12 from Wall-2

3 Results and discussion

3.1 Computed tomography (CT) radiography

Porosity measurement can be performed using optical microscopy, however, the measurement is restricted to examining surfaces and 2D planes. Results from two-dimensional object cannot accurately represent three dimensional features. Thus, the results are often subjected to errors. The CT radiography can reveal volumetric defects that increases the accuracy level of the defect detection and characterisation.

Figure 4 and Figure 5 shows CT radiographed images of Wall-1 and Wall-2 respectively and reveal increased porosity at the central part of one surface of the wall. This particular area represents all end points of weld runs. i.e. end of each weld layer and so it can be asserted that the porosity formed at this surface is weld end defect rather than a formed pore during welding. All the defects in this area are omitted from the calculations in this study. The area highlights the importance of welding parameter optimisation to avoid any defect formation. As discussed by Xiong et al. [18] and Xiong et al.[19], unlike conventional multi-pass welding, in WAAM, a uniform height of previously deposited layer which serves as a substrate for next depositing layer is of great importance. A small reduced height at the weld start and weld end cumulatively adds-up to an appreciable value after deposition of 10 to 12 layers. Thus, the uneven surface at the weld start and end compared to other parts forge weld defects that can be clearly seen from Figure 4 and Figure 5. For all other locations porosity is randomly distributed.

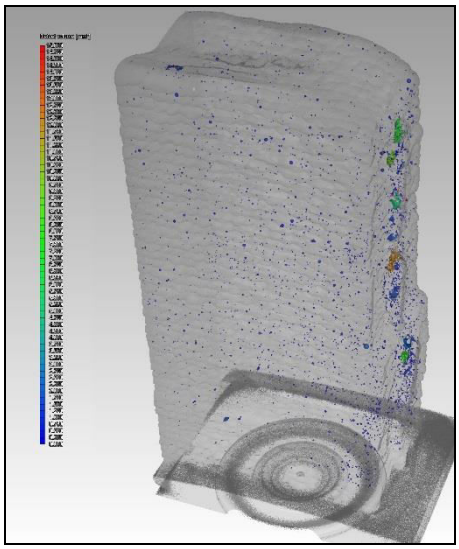

Fig. 4. CT radiography image of small part of Wall 1

From the examined wall parts, Wall-1 and Wall-2 revealed overall 0.02035% and 0.01823% porosity by volume. Clearly a lower interpass temperature of 50°C in Wall-1 possessed 10.41% more porosity than the Wall-2 prepared with 100°C. From Table 3, it is clear that the pores with volume between 0.01 to 0.05mm3 contributed around 85% of the total pores present in both the walls. The pores ranging from 0.05 to 0.15 mm3 counted

around 14% more in Wall-2 compared with Wall-1. For pore volume greater than 0.015 mm3, Wall-1 presented more percentage of pores than Wall-2. Interestingly, pores with volume greater than 0.6 mm3 were virtually absent in wall sample of higher interpass temperature. Large pores with size up to 2 mm3 in volume were observed in Wall-1 only. Considering the volumetric distribution of pores, the small sized pores (<0.015 mm3) occupied more than 81% of total volume occupied by pores in Wall-2, compared with 68% in Wall-1. In addition, in Wall-2, the pores with size 0.01 to 0.05 mm3 contributed 51% compared with 45% by volume in Wall-1. Considering the top layer of both walls, Wall-2 had more porosity than Wall-1. Interestingly, only top layer contained 13.1% of the overall porosity volume in Wall-2 dominated by small sized pores (>98%).

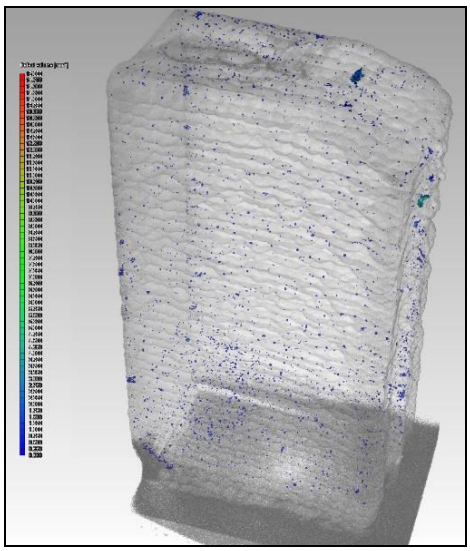

Fig. 5. CT radiography image of small part of Wall 2

Table 3. Comparison of number of pores present in the walls

Pore Volume (mm^3)	Wall 1 (50°C)		Wall 2 (100°C)	
	Vol %*	Count %^	Vol %*	Count %^
0.01 to 0.05	44.96	85.45	50.95	84.81
0.05 to 0.1	15.46	8.8	21.06	10.24
0.1 to 0.15	7.50	2.35	9.46	2.70
0.15 to 0.2	5.76	1.31	5.29	1.07
0.2 to 0.3	6.00	0.94	5.25	0.72
0.3 to 0.4	2.15	0.23	1.33	0.12
0.4 to 0.5	3.85	0.32	1.20	0.08
0.5 to 0.6	2.82	0.18	2.11	0.12
0.6 to 0.7	0.84	0.04	0	0
0.7 to 0.8	0.92	0.04	0.95	0.04
0.8 to 0.9	0	0	0	0
0.9 to 1.0	2.34	0.09	0	0
1.0 to 1.5	4.34	0.09	0	0
1.5 to 2.0	2.99	0.09	2.34	0.04

*Contribution of particular sized pores considering overall volume of pores present in respective walls
^Contribution of particular sized pores considering overall pore count in respective walls

During the solidification of the molten weld pool, dissolved atomic hydrogen in solid metal is rejected into the liquid metal depending upon the temperature and the difference in solubility limit of hydrogen in liquid and solid aluminium. The quickly formed oxide layer also absorbs hydrogen from moisture in the air. The continuously increasing hydrogen in liquid reaches to solubility limit and finally forms a pore at the grain boundary of the solidified metal. Depending upon the pore size and buoyancy force, pores are usually entrapped at the top of the fusion line [20]. A macro of the wall samples reveals increased porosity at the fusion lines (refer Figure 6)

The possibility of increased pores at the top layer could be floatation of pores layer by layer. While depositing successive layer, pores at the surface of the previous layer were taken to next layer by partial remelting and addition of new liquid metal by welding arc. The entrapped pores at the bottom of the previous layer cannot reach to the top. Also, arc forces while depositing next layer possess limited penetration where liquid metal cannot form, the entrapped porosity remains untouched that can be witnessed as increased porosity near the fusion line. The inter layer waiting time for Wall-2 was less that Wall-1. During the solidification of metal while depositing a layer, comparatively faster solidification is expected at Wall-1 than Wall-2 due to lower and higher interpass temperatures respectively. Thus, liquid metal is exposed to the air for a longer time in Wall-2 than Wall-1. Also, the solidified metal at top surface is readily exposed to the air for longer time period compared to the rest part of wall and thus, comparatively higher cooling effect is expected at the top surface. Thus, it can be inferred that the time was insufficient for coalescence and growth of the micro pores at the top layer. This could explain the presence of majority of the small sized pores at the top surface. The effect greatly increases along with wall height.

The presence of large sized pores in Wall 1 can be attributed to the classical Ostwald Ripening effect [9]. The inter-pores coalescence is expected from the micro-pores as well as hydrogen entrapment site such as grain boundaries or lattice imperfections. As explained previously, the entrapped untouched pores at the fusion line are cyclically exposed to higher and lower temperatures by successive deposition of weld layers. A time factor greatly influences the hydrogen diffusion and coarsening of pores. Pores of Wall-1 were exposed to higher temperature for longer time due to the increased inter-layer waiting time compared to Wall-2 that could have allowed hydrogen diffusion and pore coarsening. This could be the reason for the presence of large sized pores in Wall-1 which were virtually absent in Wall-2. In previous studies on pore coarsening [9], [20] a single bead wall structure was considered (wall width around 6 to 7 mm) where heat extraction is comparatively faster compared with higher width wall structures such as 45mm studied in this paper. As discussed in Section 2.2, only temperature of the top layer was the criteria for deposition of next layer, the temperature of the wall samples below 3 to 4 layers was certainly much higher than measured at the top due to heat sink effect. From

the experimental results it can be deduced that the mechanism of formation of large pore is not only a function of solubility limit and temperature alone but also a rate of heat extraction and time that facilitates the movement of entrapped dissolved hydrogen through pipes such as dislocations.

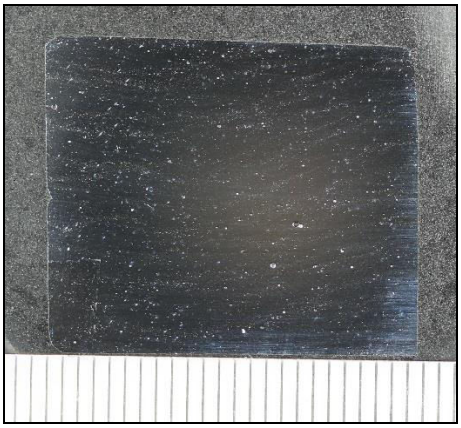

Fig. 6. Macro test specimen revealing fusion lines

In overall comparison, Wall-2 displayed reduced porosity over Wall-1. It can be said that the porosities that passed upwards through the solidifying melt to the top of the layer were disturbed by the deposition of next layer. The overall hydrogen content was more than the solubility limit so that most of the hydrogen gas was released to the air reducing overall hydrogen content in the wall sample.

3.2 Tensile testing

The 5356 weld consumable is expected to give typical tensile strength, yield strength and % elongation of 265MPa, 120 MPa and 26% respectively, based on data provided by the consumable manufacturer; however, based on the specimen locations in the WAAM walls, not all specimens showed expected properties. The filler wire 5356 is used to weld wide variety of base metals. A comparable compositional wrought products, 5083 and 5086 reveal 290 and 260 MPa tensile strength, 145 and 115 MPa yield strength and 22 % elongation respectively [21]. Figure 6 compares the ultimate tensile strengths of Wall-1 and Wall-2 in horizontal and vertical directions. From the Figure 6, all the specimens from Wall-2 revealed tensile strength higher than recommended by manufacturer, except for one specimen (specimen no. 9) that witnessed pores at the fracture surface. However, total three specimens from Wall-1 showed less strength than recommended. Horizontal specimens showed higher tensile properties than vertical specimens in both the wall samples. The average tensile strength of the horizontal specimens was 3.6 and 3.9 % more than vertical specimens for Wall-1 and Wall-2 respectively. Vertical specimens contained more fusion lines and thus increased entrapped pores, as disused in Section 3.1, than the horizontal specimens. The multiple existence of fusion lines and increased pore numbers could be the possible reason for reduced strength for the samples in vertical direction. In case of horizontal specimens, such multiple fusion lines were absent due to its parallel orientation with the direction of layer deposition (torch progression). Comparing the overall strength of the two walls, Wall-2 with higher interpass temperature showed more strength than Wall-1 with marginal difference of 4MPa. Effect of residual stress will be investigated in the future.

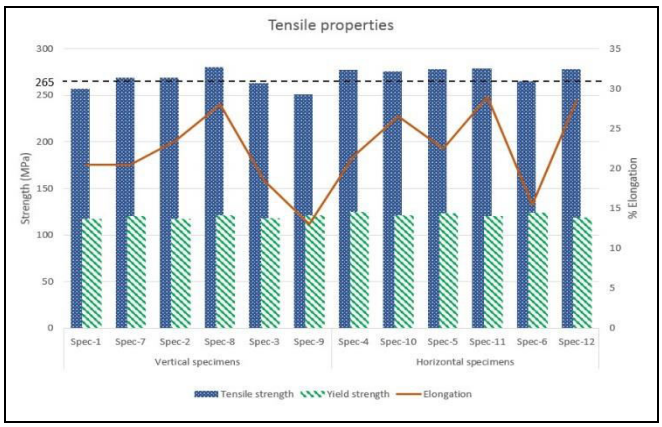

Fig. 7. Comparison of tensile strength between specimens extracted from Wall-1 (50°C, specimens 1 to 6) and Wall-2 (100°C, specimens 7 to 12)

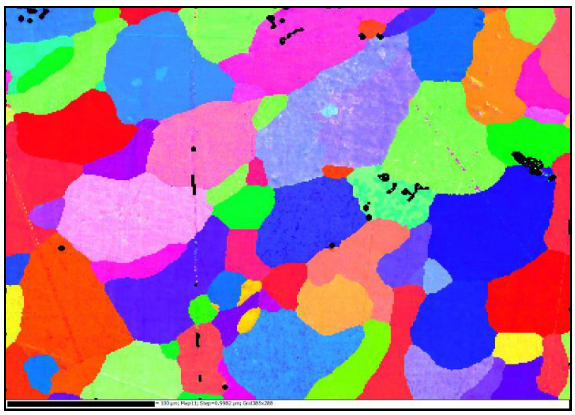

Fig. 8. Microstructure of plane normal to the torch progression of Wall-1

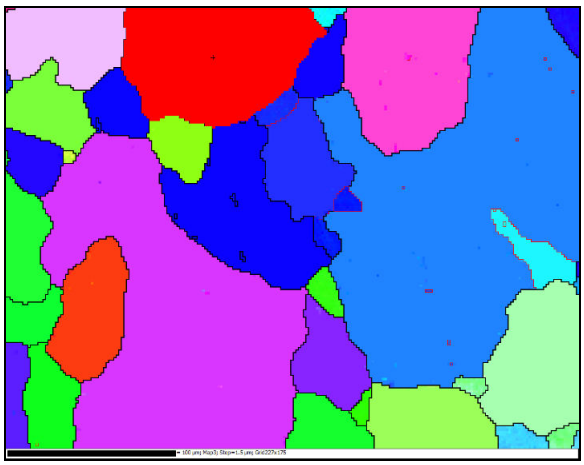

Fig. 9. Microstructure of plane normal to the torch progression of Wall-2

3.3 Microstructure

Figure 8 and Figure 9 illustrate the microstructure of the plane perpendicular to torch progression direction from Wall-1 and Wall-2 respectively. The solidification rate found to have great effect on grain size of the solidified metal. Impressively, slower solidification in Wall-2 with 100°C interpass temperature witnessed grain size 54% larger than the grains of Wall-1. Thus, comparatively, Wall-1 showed more grain boundaries than Wall-2 which is considered as one of the trapping sites for hydrogen. In addition, during solidification, dendrites provide nucleation sites for pores. It can be inferred that the presence of larger grain boundary area and the availability of suitable inter dendritic spaces were responsible for the increased porosity in Wall-1. As discussed in Section 3.1, the heat treatment effect produced during wall fabrication resulted in the coalescence of dissolved hydrogen and micro pores entrapped in the grain boundaries and dendritic arms which explains the existence of large sized pores in Wall-1. Presence of relatively less hydrogen entrapment site such as grain boundaries and release of hydrogen in to the atmosphere by arc forces could be the possible reason of existence of reduced porosity in Wall-2.

4 Conclusion

Interpass temperature in wire arc additive manufacture (WAAM) of aluminium has great effect on porosity formation. Higher interpass temperature samples revealed less pore content dominated by small sized pores compared to lower interpass temperature sample that revealed presence of large size pores. Cyclic high temperature exposure of the sample for longer time may have supported coalescence of small pores in lower interpass temperature sample. Floatation of pores from layer-by-layer and longer exposure of liquid metal to the air due to slower solidification could be the probable reason for the presence of increased porosity at the top layer in higher interpass sample. Higher interpass temperature sample and horizontal directional samples showed better tensile strength than lower interpass temperature sample and vertical specimens respectively. A large difference in the size of grains were observed between the two types of wall samples.

This publication was made possible by the sponsorship and support of Lloyd's Register Foundation and Kraken project, a Horizon 2020 project funded by European Commission (Grant Number 723759). Lloyd's Register Foundation helps to protect life and property by supporting engineering-related education, public engagement and the application of research. The present work was enabled through, and undertaken at, the National Structural Integrity Research Centre (NSIRC), a postgraduate engineering facility for industry-led research into structural integrity establishment and managed by TWI through a network of both national and international Universities.

References

1. S. W. Williams, F. Martina, A. C. Addison, J. Ding, G. Pardal, P. Colegrove, Mater. Sci. Technol., **32**, 7, 641–647 (2016)
2. J. Gu, J. Ding, S. W. Williams, H. Gu, J. Bai, Y. Zhai, P Ma, Mater. Sci. Eng. A, **651**, 18–26 (2016)
3. K. S. Derekar, Mater. Sci. Technol., **34**, 8, 1–22 (2018)
4. C. Zhang, Y. Li, M. Gao, X. Zeng, Mater. Sci. Eng. A, **711**, 415–423 (2018)
5. J. Gu, B. Cong, J. Ding, S. W. Williams, Y. Zhai, *25th Annual International Solid Freeform Fabrication Symposium,* 4-6 (2014)
6. J. Donoghue, A. A. Antonysamy, F. Martina, P. A. Colegrove, S. W. Williams, P. B. Prangnell, Mater. Charact., **114**, 103–114 (2016)
7. A. Gomez Ortega, L. Corona Galvan, F. Deschaux-Beaume, B. Mezrag, S. Rouquette, Sci. Technol. Weld. Join., **23**, 4, 316–332(2018)
8. H. Geng, J. Li, J. Xiong, X. Lin, D. Huang, F. Zhang, Rapid Prototyp. J., **24**, 2, 342–350 (2015)
9. J. Gu, J. Ding, S. W. Williams, H. Gu, P. Ma, Y. Zhai, J. Mater. Process. Technol., **230**, 26–34 (2016)
10. B. Wu, D. Ding, Z. Pan, D. Cuiuri, H. Li, Z Fei, J. Mater. Process. Technol., **250**, 304–312 (2017)
11. P. A. Colegrove, F. Martina, M. Roy, B. Szost, S. Terzi, S. W. Williams, P. Withers, D. Jarvis, Adv. Mater. Res., **996**, 694–700 (2014)
12. H. Geng, J. Li, J. Xiong, X. Lin, Sci. Technol. Weld. Join., **22**, 6, 472–483 (2017)
13. B. Wu, Z. Pan, D. Ding, D. Cuiuri, H. Li, Z. Fei, J. Mater. Process. Technol., **258**, 97–105 (2018)
14. J. Xiong, R. Li, Y. Lei, H. Chen, J. Mater. Process. Technol., **251**, 12–19 (2018)
15. G. Mathers, *The welding of aluminium and its alloys*. Woodhead Publishing Ltd, Cambridge England (2002)
16. H. Geng, J. Li, J. Xiong, X. Lin, F. Zhang, J. Mater. Eng. Perform., **26**, 2, 621–629 (2017)
17. B. Cong, Z. Qi, B. Qi, H. Sun, G. Zhao, J. Ding, Appl. Sci., 7, 3, 275 (2017)
18. J. Xiong, Z. Yin, W. Zhang, Int. J. Adv. Manuf. Technol., **87**, 1–4, 579–586 (2016)
19. J. Xiong, G. Zhang, W. Zhang, Int. J. Adv. Manuf. Technol., **80**, 9–12, 1767–1776 (2015)
20. J. Bai, H. Ding, J. Gu, X. Wang, H. Qiu, *1st International Conference on New Material and Chemical Industry (NMCI2016),* (2017)
21. ASM Handbook Committe, *Metals Handbook (Vol.2) - Properties and Selection: Nonferrous alloys and Special-purpose materials, 10th ed.* Materials Park, Ohio USA (1990)